CO_2-Induced Stereocomplex Formation of Stereoregular Poly(methyl methacrylate) and Microcellular Foams

Tomohiro Mizumoto,* Norio Sugimura, and Masahiko Moritani

Basic Chemicals Laboratory, Sumitomo Chemical Co., Ltd., 5-1, Sobiraki-cho, Niihama, Ehime 792-8521, Japan

Yoshiyuki Sato and Hirokatsu Masuoka

Department of Chemical Engineering, Faculty of Engineering, Hiroshima University, 1-4-1, Kagamiyama, Higashi-Hiroshima, Hiroshima 739-8527, Japan

Received March 10, 2000; Revised Manuscript Received June 19, 2000

ABSTRACT: Crystalline stereocomplex formation of isotactic poly(methyl methacrylate) (*it*-PMMA) and syndiotactic poly(methyl methacrylate) (*st*-PMMA) induced by high-pressure CO_2 at pressures in the 5−35 MPa range and at temperatures in the 30−110 °C range was demonstrated by means of differential scanning calorimetry (DSC) and wide-angle X-ray scattering (WAXS) investigations as a function of treatment pressure, temperature, and the *it*-PMMA/*st*-PMMA ratio. At a constant *it*-PMMA/*st*-PMMA ratio, the melting temperature of the stereocomplexes was shown to increase with increasing treatment pressure and temperature. The amount of the stereocomplex formed by high-pressure CO_2 was found to be higher than that by thermal annealing in bulk. The heat of melting of the stereocomplex was the highest for the 1/2−1/1 *it*-PMMA/*st*-PMMA ratio. Compared with amorphous PMMA, the crystalline stereocomplex induced by high-pressure CO_2 contributes to the superior morphology of the microcellular foams obtained. For the CO_2-treated polymer, the average cell size decreases and the average cell density increases as the amount of the stereocomplex that was formed increases.

Introduction

Since the first report of Fox et al.[1] in 1958, stereocomplex formation between isotactic poly(methyl methacrylate) (*it*-PMMA) and syndiotactic poly(methyl methacrylate) (*st*-PMMA) has been investigated by turbidity,[2−5] light scattering,[6−10] sedimentation,[11] osmometry,[10,12] GPC,[10,13] viscometry,[4−7,9,10,14−17] DSC,[5,18−26] X-ray diffraction,[3,5,11,17,18,20−22,27−29] NMR,[5,17,30−34] IR spectroscopy,[34,35] dynamic mechanical measurement,[18,36,37] and nonradiative energy transfer (NET).[38,39] These studies have been reviewed by Spevacek et al.[34,40] and te Nijenhuis.[41] The stereocomplex formation between *it*-PMMA and *st*-PMMA occurs in organic solvents, and the solvents have been observed to have a considerable influence on the stereocomplex formation. The solvents for complex formation can be divided into three groups: strongly complexing solvents (e.g., acetone, tetrahydrofuran), weakly complexing solvents (e.g., toluene, benzene), and non-complexing solvents (e.g., chloroform, dichloromethane).[4] The formation of the stereocomplex between *it*-PMMA and *st*-PMMA is also known to occur in bulk thermal annealing as well as in organic solvents: after annealing between 130 and 160 °C. For this case, the melting endotherm can be observed at about 190 °C, even with samples precipitated from a non-complexing solvent.[2,5,18,20,23,28] However, the formation of the complex in the bulk is a less favorable process than that in dilute solutions, since the maximum degree of crystallinity formed by thermal annealing is half as much as that induced by organic solvents.

Although suitable ratios of *it*-PMMA to *st*-PMMA for stereocomplex formation have been reported in the literature, the precise conditions are still not completely clear at present.[40,41] According to Schomaker et al.,[19,42] the stereocomplex nuclei formation is a consequence of the contact between one *it*-PMMA chain and one *st*-PMMA chain at the very start of process. Subsequently, these complex nuclei can initiate an aggregation process at a ratio of *it*-PMMA/*st*-PMMA = 1/2 on the monomeric level. Hatada et al. observed stereocomplex formation process precisely using conventional GPC,[43,44] using uniform *it*-PMMA and *st*-PMMA, which had been isolated by means of preparative supercritical fluid chromatography. Their results indicate that the initial stage of stereocomplex formation involves the association of a single molecule of *it*-PMMA and a single molecule of *st*-PMMA. On the other hand, DSC and WAXS indicate that the melting point and the crystalline structure of the stereocomplexes formed in the bulk or in organic solution are independent of the *it*-PMMA to *st*-PMMA ratio of the initial mixture[5,20] and, therefore, that there is only one type of stereocomplex. Kusanagi et al. have suggested that the structure of the stereocomplex is closely related to the double-stranded helix conformation of *it*-PMMA.[27] Bosscher et al. came to the conclusion that the stereocomplex consists of a double-stranded helix with a 60/4 helical conformation.[28,45] Furthermore, on the basis of fiber diffraction patterns, the stereocomplex is made of a 9/1 double-stranded helix with an asymmetric unit consisting of one *it*-PMMA unit and two *st*-PMMA units. It is interesting to note that this conformation is very close to the conformation of pure *it*-PMMA with a 10/1 helix structure[27,45] and that of *st*-PMMA with a 74/4 helix.[29]

On the other hand, *it*-PMMA and *st*-PMMA prepared by conventional free radical polymerization form a stereocomplex with a low melting temperature.[40,41,46] Allen et al.[37] compared the crystallization behavior of blends of *it*-PMMA with *st*-PMMA or atactic PMMA (*at*-PMMA) induced by some solvents or by thermal treatment and measured the crystallinity and the dynamic

10.1021/ma000443n CCC: $19.00
Published on Web 08/18/2000

mechanical properties of such blends. In many cases when using samples of low stereoregularity, an apparent stoichiometric ratio was found for a ratio of *it*-PMMA and *st*-PMMA that is close to 1/1.[41]

Supercritical fluids have attracted the attention of chemical engineers for many years because of their highly adjustable solvent properties, such as high diffusivity and low viscosity. The advantages of using supercritical fluids in polymer engineering as polymerization solvents and foaming agents include their ability to plasticize many polymers and dissipate energy during the process. Carbon dioxide is nonflammable, nontoxic, and relatively inexpensive and has a moderate critical temperature and pressure ($T_c = 31.1$ °C, $P_c = 7.38$ MPa), which make it a convenient for many applications. The application of supercritical CO_2 in microcellular foaming processes is an area of significant research activity. Microcellular foams are plastics with small cell sizes on the order 10 μm in diameter and large cell densities of the order of 10^9 cells/cm^3. Microcellular foams have been studied for polymers such as poly(ethylene terephthalate) (PET),[47−54] polystyrene,[55−58] poly(vinyl chloride),[59−63] poly(methyl methacrylate) (PMMA),[47,64] and polycarbonate.[65,66] Microcellular foams are known to exhibit high impact strength, high toughness, and a long fatigue life. The basic procedure to produce microcellular foam is a two-stage process. In the first stage, a polymer sample is placed in a high-pressure, nonreactive gas, such as CO_2 and N_2, environment at a temperature below the glass transition temperature, T_g, and allowed to absorb the gas. In the second stage, the pressure is released, and the polymer sample foams due to supersaturation in the polymer and CO_2 solution.

Although supercritical CO_2 is a weak solvent for polymers with exception of some fluoropolymers and silicones, it can plasticize glassy polymers by reducing the T_g. Chiou et al. have reported on the plasticizing effect of CO_2 dissolved in PET and the resulting crystallization. Their results indicate that in the presence of CO_2 the T_g decreases, and further, at large contact times, CO_2 leads to a higher degree of crystallinity.[67] Mizoguchi et al. have reported that the crystallization rates of PET in high-pressure CO_2 were faster than that for thermal treatment above T_g.[68] Similar investigations have been reported for bisphenol A polycarbonate,[69] poly(phenylene sulfide),[70] poly(aryl ether ether ketone),[71] and polystyrene.[72−74] These studies show that supercritical fluids can induce crystallinity below T_g and that the crystallization rate increases with temperature and pressure. Further, the level of crystallinity is comparable with that induced by organic solvents.[71]

Baldwin et al. and Kumar et al. have reported on the crystallization of PET due to sorption of CO_2 during microcellular processing.[49,51−53] The CO_2-induced crystallinity in PET is the dominant factor affecting bubble nucleation and growth in the PET microcellular foams obtained. Crystalline polymers are relatively difficult to use in microcellular process compared with amorphous polymers since CO_2 does not dissolve in the crystalline region.[53] However, crystallized PET shows small cell sizes and large cell densities. Carbon dioxide-induced crystallization has been found to play a major role in the microcellular processing through its effects on (a) the cell nucleation mechanism resulting in larger cell densities due to heterogeneous nucleation at the amorphous/crystalline boundaries and (b) the cell growth mechanism resulting in smaller cell sizes due to the increased matrix stiffness of the crystalline matrix.[49,51−53] On the other hand, uniform microcellular structures have hardly been studied in high-density polyethylene and polypropylene because of the nonuniform crystalline morphology. For the case of blended samples of polyethylene and polypropylene, microcellular foams have been found to produce a uniform structure because of the fine crystalline structure.[75,76]

Table 1. Characteristics of the Polymer Samples

			tacticity (%)[b]		
sample	$10^{-4}M_n$[a]	M_w/M_n[a]	mm	mr	rr
it-PMMA	3.62	10.06	81.0	9.6	9.4
st-PMMA	5.58	1.93	6.7	36.1	57.2

[a] Measured by GPC with *at*-PMMA standards calibration. [b] Calculated by ^{1}H NMR.

The first part of this study deals with the stereocomplex formation between *it*-PMMA and *st*-PMMA blends in high-pressure CO_2 and mainly in supercritical CO_2. We investigated the extent of the stereocomplex formation in high-pressure CO_2 by means of differential scanning calorimetry (DSC) and wide-angle X-ray scattering (WAXS) as a function of crystalline condition, such as CO_2 treatment pressure, temperature, and the ratio of *it*-PMMA/*st*-PMMA. In the second part of the study deals with the relationship between the crystalline stereocomplex formed by high-pressure CO_2 and the resulting microcellular morphologies. Compared with amorphous PMMA, the effect of the crystalline structure in PMMA on the microcellualar morphologies such as the average cell size and the average cell density was studied.

Experimental Section

Materials. The *it*-PMMA sample was prepared by an anionic polymerization technique.[77] The *st*-PMMA sample was prepared by a conventional free radical polymerization technique. Molecular weight (M_n) and molecular weight distribution (M_w/M_n) were measured by gel permeation chromatography (GPC) at 40 °C with a Waters GPC 150-CV apparatus equipped with Shodex KF-800L, KF-806L, KF-805L, KF-804L, KF-803L, and KF-801 GPC columns. THF was the eluent (flow rate of 1 mL/min), and *at*-PMMA standards ($M_w/M_n < 1.10$, Polymer Laboratories) were used for calibration. The GPC chromatograms were recorded using refractive index detector. ^{1}H NMR spectroscopy were taken on a Varian XL-200 spectrometer at 200 MHz in nitrobenzene-d_5 at 110 °C. Tacticities, the content of isotactic (mm), heterotactic (mr), and syndiotactic (rr) triads, were derived from integrated intensities of the α-CH_3 peaks at 1.50 ppm (mm), 1.34 ppm (mr), and 1.22 ppm (rr) in 2 wt % solutions of polymers. The molecular weight, the molecular weight distribution, and the tacticity of prepared PMMAs are listed in Table 1.

The amorphous PMMA film was prepared by solution casting. The *it*-PMMA and *st*-PMMA (desired *it*-PMMA/*st*-PMMA ratio of 50/50 (wt %/wt %)) were dissolved in dichloromethane. The 30 wt % solution was cast on a poly(ethylene terephthalate) (PET) film, and most of the solvent was allowed to evaporate at 40 °C for 20 min. The resulting film was removed from PET film and dried for 1 day at room temperature under vacuum. The film obtained had a smooth surface and was about 110 μm in thickness. The amorphous PMMA sheets with a thickness of about 600−1500 μm was prepared by melt pressing. The *it*-PMMA and *st*-PMMA were melt mixed in a resin kneading machine preheated to 240 °C at various mixing ratios. The blend mixtures obtained were pressed for 6 min at 220 °C and were cooled slowly down to room temperature.

High-Pressure CO_2 Treatment and Microcellular Processing Procedure. For high-pressure CO_2 treatment and

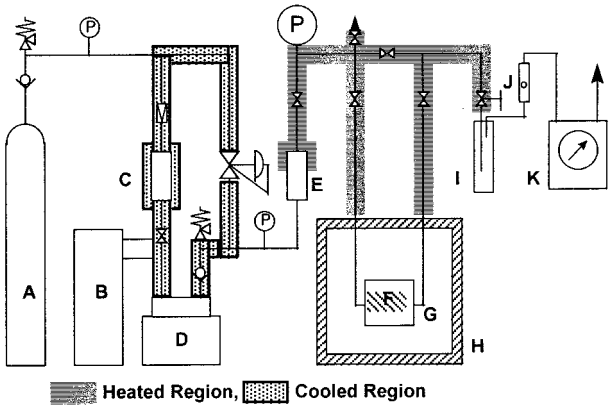

Figure 1. High-pressure apparatus for treating polymer films: A, CO_2 cylinder; B, cooler; C, reservoir; D, pump; E, buffer tank; F, polymer film; G, autoclave; H, air bath; I, trap; J, flow meter; K, gas meter.

the microcellular processing, a stainless steel autoclave (40Φ × 27 mm) equipped with a pressure gauge was used as a polymer sample cell (Figure 1). The cell was placed in a thermostatically controlled air bath. High-pressure CO_2 treatment of the amorphous PMMA films was carried out with the following procedure. First, after the sample (20 × 20 mm) was loaded into the autoclave, then air was removed from the apparatus by purging with CO_2. The sample was exposed to high-pressure CO_2 at a desired pressure ranging from 5 to 35 MPa. The autoclave was maintained at the desired temperature for a given period of time. The time for introducing CO_2 was several minutes, and the CO_2 depressurization rate was 5 MPa/h, which was controlled with a flow meter. By using this procedure, the sample obtained was a transparent film without any visible bubbles.

The microcellular processing was carried out as follows. Amorphous PMMA prepared by the melt press method was contacted with high-pressure CO_2 using the high-pressure CO_2 treatment procedure outlined above. After the treatment time had elapsed at the desired conditions, the autoclave was depressurized over several seconds. For this case, the sample obtained was a translucent film with many small visible bubbles.

Analysis. Differential scanning calorimetry (DSC) was carried out with a Seiko SSC-580II instrument that was calibrated with indium. After loading each sample into the DSC, the temperature was brought to 0 °C and maintained at that temperature for 5 min. The thermograms were recorded at a heating rate of 10 °C/min. The melting temperature, T_m, was determined from the maximum of the melting endotherm. The heat of melting, ΔH, was determined by the peak area of the melting endotherm. Wide-angle X-ray scattering (WAXS) measurements were carried out on a Rigaku RINT2100 apparatus with a Cu Kα radiation (40 kV × 40 mA) in 2θ transmission mode within the range of 2θ from 2° to 90°.

The characterization of the foamed samples was performed using a scanning electron microscope (SEM). The SEM samples were prepared by fracturing the obtained foam samples and gold sputtering the fractured cross sections. The SEM used was a JEOL JSM840A apparatus with acceleration voltage being in the range from 5 to 7 kV. The average cell size, D, was statistically calculated from SEM micrographs by an image analyzer (Toyobo image analyzer V10LAB). The average cell density, N, represents the average number of cells per unit volume of the obtained foam samples. Equation 1 was used to calculate the average cell density, where A is the area of the statistically analyzed domain and n is the number of cells in A.

$$N = \frac{\left(\frac{n}{A}\right)^{3/2}}{1 - \frac{4}{3}\pi\left(\frac{D}{2}\right)^3\left(\frac{n}{A}\right)^{3/2}} \qquad (1)$$

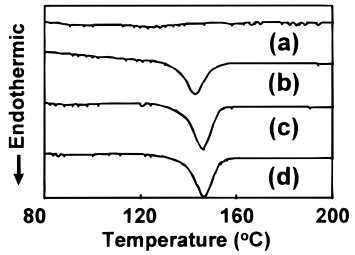

Figure 2. DSC thermograms of *it*-PMMA/*st*-PMMA (50/50) blend films treated with high-pressure CO_2 at 50 °C and 20 MPa for (a) 0, (b) 1, (c) 6, and (d) 12 h. Heating rate 10 °C min^{-1}.

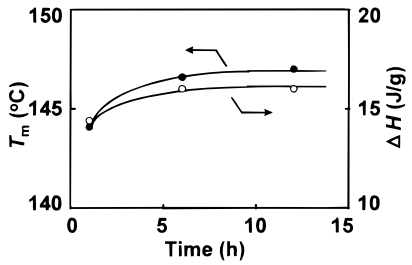

Figure 3. T_m and ΔH of the stereocomplex melting of the *it*-PMMA/*st*-PMMA (50/50) blend films as a function of treatment time at 50 °C and 20 MPa: T_m (●); H (○).

Results and Discussion

CO_2-Induced Stereocomplex Formation of *it*-PMMA/*st*-PMMA Blend Films. Figure 2 shows the DSC thermograms of the *it*-PMMA/*st*-PMMA (50/50 wt/wt) blend films treated with CO_2. The DSC thermogram of the untreated sample had a very small endothermic peak ($\Delta H = 0.4$ J/g) with a maximum at 122.8 °C. This endothermic peak near T_g is probably due to the enthalpy of relaxation. On the other hand, the thermograms of the samples treated for 1−12 h exhibited large endothermic peaks ($\Delta H \sim 16$ J/g) with maxima at about 147 °C. Stereocomplexes consisting of *it*-PMMA with low stereoregularity (mm = 80−83%)/*st*-PMMA with low stereoregularity (rr = 55−77%) had only one strong endotherm at 150−162 °C.[46,78] These large endothermic peaks, consequently, correspond to the heat of melting of the stereocomplex induced by high-pressure CO_2. Figure 3 gives T_m and ΔH of melting of the stereocomplex as a function of treatment time. There is a slight increase in T_m and ΔH over a period of about 6 h at these conditions. The rate of the stereocomplex formation is high at short treatment times and tends toward zero for times longer than 6 h. These results demonstrate that the treatment of *it*-PMMA/*st*-PMMA blends with high-pressure CO_2 causes the formation of stereocomplex.

Figure 4 shows WAXS patterns of the *it*-PMMA/*st*-PMMA blend films. The crystalline films, which had large endothermic peaks at about 147 °C, had a reflection at $2\theta = 11°$, in agreement with previous observations by Challa et al.[3,18] for *it*-PMMA/*st*-PMMA stereocomplexes. No reflection at $2\theta = 11°$ was observed for the untreated amorphous *it*-PMMA/*st*-PMMA blend. Furthermore, the reflection at $2\theta = 8.6°$, corresponding to *it*-PMMA crystalline structure,[22] was not observed on the WAXS patterns for the *it*-PMMA/*st*-PMMA blend films regardless of treatment with CO_2. WAXS provides additional evidence for the crystalline stereocomplex of *it*-PMMA/*st*-PMMA induced by high-pressure CO_2.

Figure 5 depicts the DSC thermograms of the stereocomplex for the *it*-PMMA/*st*-PMMA blend films obtained

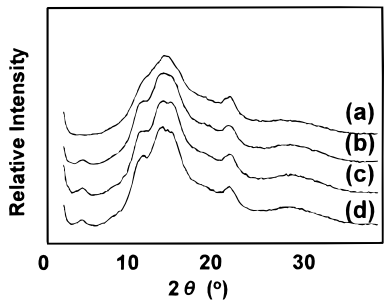

Figure 4. Smoothed X-ray diffraction patterns of *it*-PMMA/*st*-PMMA (50/50) blend films treated with high-pressure CO_2 at 50 °C and 20 MPa for (a) 0, (b) 1, (c) 6, and (d) 12 h.

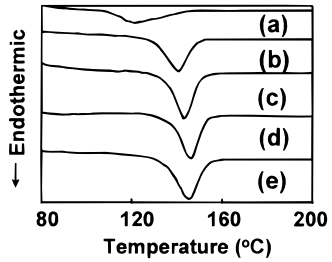

Figure 5. DSC thermograms of *it*-PMMA/*st*-PMMA (50/50) blend films treated with high-pressure CO_2 at 50 °C for 6 h at (a) 5, (b) 10, (c) 15, (d) 20, and (e) 25 MPa. Heating rate 10 °C min^{-1}.

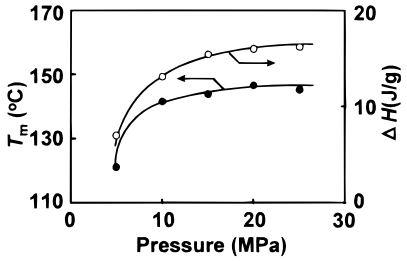

Figure 6. T_m and ΔH of the stereocomplex melting of the *it*-PMMA/*st*-PMMA (50/50) blend films as a function of treatment pressure at 50 °C for 6 h: T_m (●); H (○).

at 50 °C for 6 h at treatment pressure indicated. For the case of treatment at 5 MPa, the sample obtained had a small endothermic peak with low T_m = 125 °C. Above 10 MPa, the samples had large endothermic peaks with a higher T_m. The T_m and ΔH of melting of the stereocomplex as a function of treatment pressure are shown in Figure 6. The T_m and ΔH of the stereocomplex increases with increasing treatment pressure at the given experimental conditions. High-pressure CO_2, particularly supercritical fluid CO_2, can lower T_g by up to 20−30 deg or more.[72] Winssinger et al. reported direct experimental determinations of T_g for PMMA in the presence of CO_2 at elevated pressure by means of a creep compliance measurement. Their results indicate that the T_g of PMMA decreased with the amount of CO_2 sorbed increasing.[79] Furthermore, they classified polymer−CO_2 systems into four fundamental types of T_g versus pressure behavior as a function of three factors: the solubility of the compressed fluid in the polymer, the flexibility of the polymer molecule, and the critical temperature of the pure solvent gas. The PMMA−CO_2 system exhibits type IV behavior, which is characterized by a pressure maximum above the critical temperature of the fluid as stated earlier.[80] According to the literature, the PMMA−CO_2 system at 5 MPa and 50 °C is in the glassy state, and the PMMA−CO_2 system above 10 MPa and 50 °C is in the liquid state. It was known that the critical sequence lengths for stereocomplex nuclei formation depended on the annealing temperature and that the critical sequence length at lower annealing temperature was smaller than that at higher annealing temperature.[23] If the critical sequence length depended on the mobility of *it*-PMMA and *st*-PMMA chains, in high-pressure CO_2 treatment, the critical sequence length at lower treatment pressure was smaller than that at higher treatment pressure. And the nucleation seems to occur faster at lower treatment pressures, and therefore many small complexes are formed.

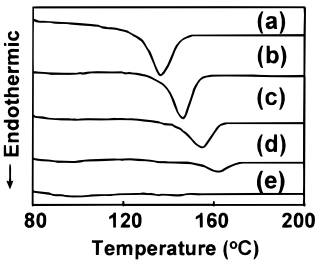

Figure 7. DSC thermograms of *it*-PMMA/*st*-PMMA (50/50) blend films treated with high-pressure CO_2 at 20 MPa for 6 h at (a) 30, (b) 50, (c) 70, (d) 90, and (e) 110 °C. Heating rate 10 °C min^{-1}.

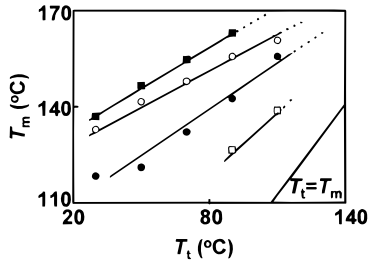

Figure 8. Hoffman−Weeks plots of the stereocomplex of the *it*-PMMA/*st*-PMMA (50/50) blend films treated with high-pressure CO_2: 5 MPa (●); 10 MPa (○); 20 MPa (■); ambient pressure in the air (□).

The DSC thermograms of the resulting stereocomplex blend films treated at different temperatures are depicted in Figure 7. In the range 30−90 °C, one large endothermic peak at about 138−164 °C was observed. Above 110 °C, no endothermic peaks could be detected. Figure 8 shows a comparison between the treatment temperature, T_t, and T_m of *it*-PMMA/*st*-PMMA with Hoffman−Weeks plots. For the case of thermal annealing, T_m is found to be linearly dependent on T_t with a slope of 0.87. A slope near unity is indicative of nonlamellar microcrystallites, such as fringed micellar crystallites. It is well-known that multiple endotherms, or so-called T_m^1, T_m^2, and T_m^3, have been reported in the literature for blends of high stereoregular *it*-PMMA (mm > 91%)/*st*-PMMA (rr > 88%).[20,23,24,81] Several explanations have been proposed, such as melting of the solvent-stabilized *st*-PMMA crystallites (T_m^1) followed by melting of stereocomplex crystallites (T_m^3)[20] or disintegration of aggregates of stereocomplex particles followed by melting of these particles.[81] Schomaker and Challa[23,24] have investigated this phenomenon in detail and proposed the occurrence of two crystallization modes. They suggested that $T_m^1 \sim 175$ °C corresponds to the melting of complexed sections partly organized into small fringed micellar clusters of the complexed sections and that $T_m^3 \sim 186$ °C corresponds to the melting of lamellar crystallites of the complexed sections. According to their works, the superheating char-

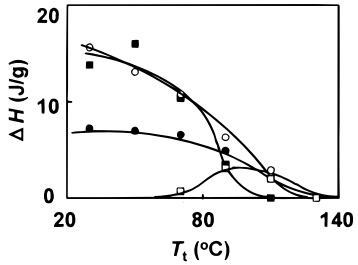

Figure 9. Relationship between ΔH of the stereocomplex for the *it*-PMMA/*st*-PMMA (50/50) blend films treated with high-pressure CO_2 and T_t: 5 MPa (●); 10 MPa (○); 20 MPa (■); ambient pressure in the air (□).

acteristics of the two types of crystallites are different since T_m of the fringed micellar crystallites increases with the heating rate in contrast to T_m of the lamellar crystallites, which is essentially independent of heating rate.[23,82] In this study, the stereoregularities of the PMMA used, *it*-PMMA and *st*-PMMA, are low (Table 1). It is probable that small fringed micellar-type crystals were induced by high-pressure CO_2 and that the hindering by the irregular sequence of each sample prevented the formation of large lamellar-type crystals and the formation of fringed micellar-type crystals with T_m above 175 °C. For high-pressure CO_2 treated samples at 5−20 MPa, T_m was found to be linearly dependent on T_t as well as that by thermal annealing (Figure 8). However, these slopes were approximately 0.5, which were different from those obtained by thermal annealing. The crystalline structure induced by high-pressure CO_2 is not clear from our results.

Figure 9 shows a plot of ΔH as a function of treatment temperature compared with the bulk annealing method at different conditions for 6 h. For thermal annealing, ΔH, which depends on the T_t, have a maximum of 4.6 J/g at 90 °C treatment. Above 130 °C, no endotherm could be detected, indicating a lack of stability of the stereocomplex of *it*-PMMA/*st*-PMMA by thermal annealing. For the case of 5 MPa, the ΔH is almost 7.0 J/g higher than the thermal annealing value. At the higher treatment pressures, 10 and 20 MPa, the ΔH is more than 10 J/g. The ΔH of melting of the stereocomplexes formed by high-pressure CO_2 treatment decreases with increasing treatment temperature. In the experimental condition, ΔH have a maximum value of about 16 J/g at lower treatment temperature, such as 30 or 50 °C. Stereocomplex formation occurs in organic solvents as well as in bulk thermal annealing as described above. The ΔH of melting of the stereocomplex induced by a suitable organic solvent is twice as large as that by thermal annealing. Our results seem to show that stereocomplexes induced by high-pressure CO_2 are comparable with those induced by organic solvents. Kazarian et al. reported that the polymers possessing electron-donating functional groups exhibit specific interactions with CO_2, most probably of a Lewis acid−base nature.[83] Recently, Bistac et al. reported that the ability of a solvent to promote stereocomplex formation depends on the solvent's basicity. In other words, PMMA does not favor polymer self-association in acidic solvents, whereas PMMA promotes polymer self-association in basic solvents.[84] Our results indicated that high-pressure CO_2 is probably a strongly or weakly complexing solvent, although high-pressure CO_2 acts as a Lewis acid.

Microcellular Foams. The amorphous PMMA foams are composed of *st*-PMMA only, whereas the crystalline PMMA foams are composed of mixtures of *it*-PMMA and *st*-PMMA at various ratios. All mixtures of *it*-PMMA and *st*-PMMA were confirmed with DSC to contain no crystalline structure prior to treatment with high-pressure CO_2. Figure 11 shows that the micrographics of *st*-PMMA and *it*-PMMA/*st*-PMMA mixture microcellualar foams processed at the given conditions. The surface of the resulting foams had a skin layer of about 10 μm in thickness. It was assumed that this skin layer is formed by phase separation of the CO_2 dissolved in PMMA during the depressurization. The inside of the microcellular foams obtained has homogeneous morphology, independent of the depth from the surface. The experimental treatment time of 5 h seemed to be sufficient for the foaming procedure at the given experimental conditions. The average cell size, D, and the average cell density, N, of the microcellular foam obtained from the *st*-PMMA sheet are 1.76 μm in diameter and 9.5×10^{10} cells/cm^3, respectively. No endothermic peak corresponding to the melting of the

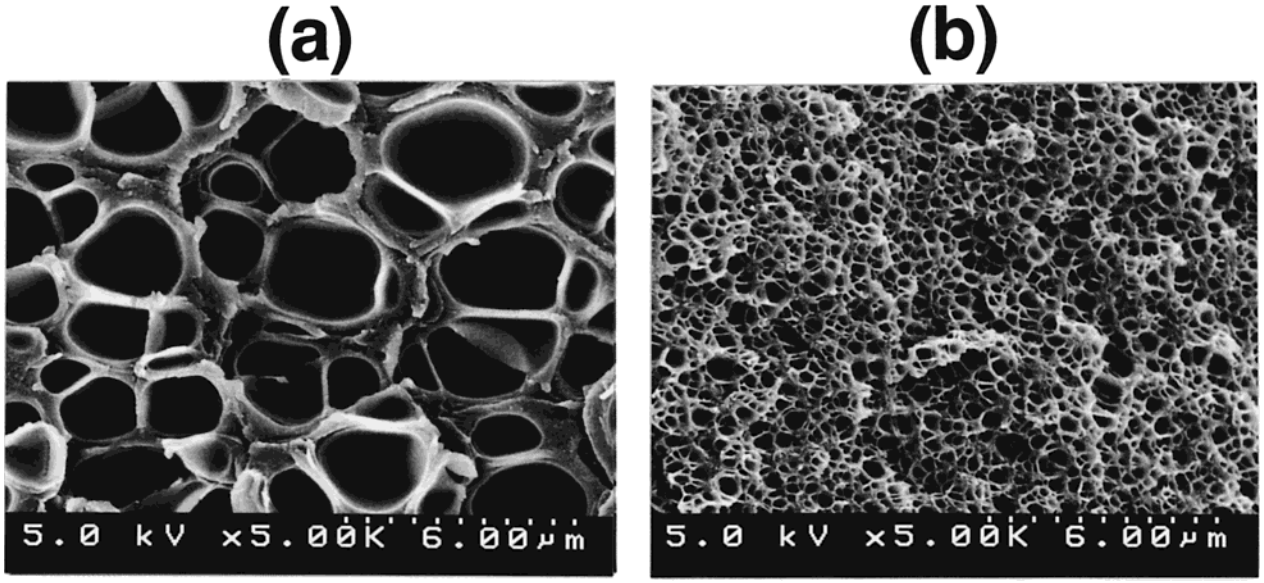

Figure 10. Micrographics of amorphous and crystalline microcellular PMMA foams processed at 35 MPa and 60 °C for 5 h: (a) *it*-PMMA = 0 wt %, $D = 1.76$ μm, $N = 9.5 \times 10^{10}$ cells/cm^3; (b) *it*-PMMA = 33 wt %, $D = 0.26$ μm, $N = 2.1 \times 10^{13}$ cells/cm^3.

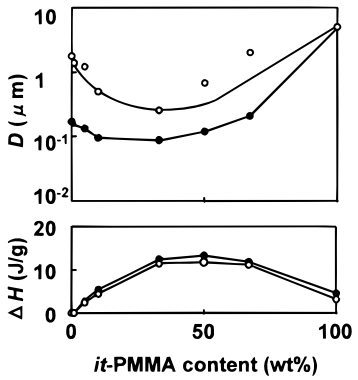

Figure 11. ΔH and D of microcellular foams obtained from the *it*-PMMA/*st*-PMMA blend sheets as a function of *it*-PMMA content at 35 MPa for 5 h: 40 °C (●); 60 °C (○).

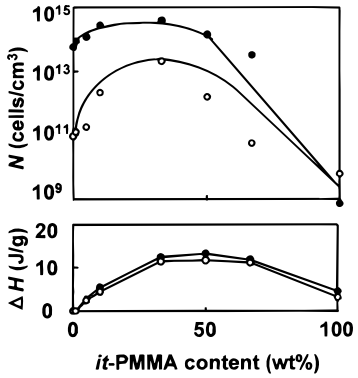

Figure 12. ΔH and N of microcellular foams obtained from the *it*-PMMA/*st*-PMMA blend sheets as a function of *it*-PMMA content at 35 MPa for 5 h: 40 °C (●); 60 °C (○).

stereocomplex was detected with the DSC thermograms. In contrast, D and N of the microcellular foam obtained from the *it*-PMMA/*st*-PMMA mixture sheet with 33% *it*-PMMA content are 0.26 μm in diameter and 2.1×10^{13} cells/cm^3, respectively. The resulting microcelluar foams have a large endothermic peak at 156.0 °C. These results indicate that the crystalline stereocomplex formed in high-pressure CO_2 contributes to the superior morphology of the microcellular foams obtained. According to Baldwin et al. in the PET−CO_2 systems, the crystalline structure plays a major role in microcellular processing through its effects on the cell nucleation mechanisms and the cell growth mechanisms.[49,51−53] In the PMMA−CO_2 systems, similarly, the stereocomplex crystalline structure formed in the microcellular processing resulted in smaller cell sizes and larger cell densities of the microcellular foams. In particular, since stereocomplex formation from the *it*-PMMA/*st*-PMMA blends occurs by high-pressure CO_2, we expect that the *it*-PMMA/*st*-PMMA makes a gel or some network structure that creates a highly viscous solution. In addition, the microcellular foam had a uniform structure because of the small fringed micellar structure.

Figures11 and 12 show the effect of *it*-PMMA content on D and N of the microcellualar foams obtained from the amorphous *it*-PMMA/*st*-PMMA blend sheets at 35 MPa for 5 h. Each figure also depicts the relationship between ΔH and *it*-PMMA content. In the range of 33−50% of *it*-PMMA content, ΔH of the resulting microcellular PMMA has a maximum at each treatment temperature. For the stereocomplex consist of low stereoregular PMMAs, as described above, it is generally accepted that the apparent stoichiometric ratio of *it*-PMMA/*st*-PMMA is 1/1 molar ratio; that is, the suitable content of *it*-PMMA is 50%.[41] For the case of the stereocomplex formation induced by high-pressure CO_2, a suitable content of *it*-PMMA is from 33 to 50% at this experimental condition, which is similar for organic solvents or bulk thermal annealing. For these *it*-PMMA contents, D and N of the resulting microcellular PMMA have a minimum and the maximum, respectively. These results provide strong evidence on the crystalline stereocomplexes induced by the high-pressure CO_2 which leads to superior morphology of the microcellular PMMA.

Conclusions

Crystalline stereocomplex of *it*-PMMA and *st*-PMMA blends formed by treatment with high-pressure CO_2 were investigated by means of DSC and WAXS measurements as a function of treatment pressure, temperature, and *it*-PMMA/*st*-PMMA mixing ratio. In the experimental condition, ΔH had a maximum value about 16 J/g at lower treatment temperature, such as 30 or 50 °C, and T_m had a maximum value about 164 °C at higher treatment pressure at above 20 MPa. If the critical sequence length depended on the mobility of *it*-PMMA and *st*-PMMA chains, in high-pressure CO_2 treatment, the critical sequence length at lower treatment pressure was smaller than that at higher treatment pressure. And the nucleation seems to occur faster at lower treatment pressures, and therefore many small complexes are formed. Hoffman−Weeks plots, however, do not show whether the crystalline stereocomplex of the *it*-PMMA/*st*-PMMA blends formed by high-pressure CO_2 are small fringed micellar structures or not. According to the classification proposed by Challa et al., high-pressure CO_2 in the pressure 5−35 MPa and the temperature 30−110 °C is a strongly or weakly complexing solvent for stereocomplex formation of poly(methyl methacrylate). Suitable ratios of *it*-PMMA/*st*-PMMA are 1/2−1/1, in agreement with stereocomplexes formed in some solvents and in bulk thermal annealing.

Compared with the amorphous PMMA foams obtained from the *st*-PMMA sheet, the crystalline stereocomplex PMMA contributes to the superior morphology of microcellular foams. The D and N obtained from the *it*-PMMA/*st*-PMMA blends are less than 0.1 μm average diameter and more than 10^{14} cells/cm^3 at 35 MPa and 40 °C for 5 h, respectively. The D decreases and N increases as the amount of stereocomplex PMMA increases.

Acknowledgment. The authors thank Mr. Takashi Kusakari at Hiroshima University for his technical assistance.

References and Notes

(1) Fox, T. G.; Carrett, B. S.; Goode, W. E.; Gratch, S.; Kincaid, J. F.; Spell, A.; Stroupe, J. D. *J. Am. Chem. Soc.* **1958**, *80*, 1768−69.
(2) Liquori, A. M.; Anzuino, G.; Coiro, V. M.; D'Alagni, M.; De Santis, P.; Savino, M. *Nature* **1965**, *206*, 358−362.
(3) Buter, R.; Tan, Y. Y.; Challa, G. *J. Polym. Sci., Polym. Chem. Ed.* **1973**, *11*, 2975−2989.
(4) Challa, G.; de Boer, A.; Tan, Y. Y. *Int. J. Polym. Mater.* **1976**, *4*, 239−249.
(5) Vorenkamp, E. J.; Bosscher, F.; Challa, G. *Polymer* **1979**, *20*, 59−64.
(6) Liquori, A. M.; De Santis Savino, M.; D'Alagni, M. *Polym. Lett.* **1966**, *4*, 943−945.
(7) Katime, I. A.; Quintana, J. R.; Strazielle, C. *Makromol. Chem.* **1986**, *187*, 1441−1455.

(8) Katime, I.; Quintana, J. R.; Veguillas, J. *Eur. Polym. J.* **1985**, *21*, 1075−1079.
(9) Bel′nikevitch, N. G.; Mrkvickova, L.; Quadrat, O. *Polymer* **1983**, *24*, 713−718.
(10) Vorenkamp, E. J.; Challa, G. *Polymer* **1981**, *22*, 1705−1708.
(11) Miyamoto, T.; Inagaki, H. *Polym. J.* **1970**, *1*, 46−54.
(12) Katime, I.; Ochoa, J. R. *Makromol. Chem., Rapid Commun.* **1982**, *3*, 783−785.
(13) Katime, I. A.; Quintana, J. R. *Makromol. Chem.* **1988**, *189*, 1373−1385.
(14) Liu, H. Z.; Liu, K. J. *Macromolecules* **1968**, *1*, 157−162.
(15) Schomaker, E.; Vorenkamp, E. J.; Challa, G. *Polymer* **1986**, *27*, 256−260.
(16) Quadrat, O.; Belnikevitch, N. G. *Polymer* **1983**, *24*, 719−721.
(17) Borchard, W.; Pyrlik, M.; Rehage, G. *Makromol. Chem.* **1971**, *145*, 169−188.
(18) Feitsma, E. L.; de Boer, A.; Challa, G. *Polymer* **1975**, *16*, 515−519.
(19) Schomaker, E.; ten Brinke, G.; Challa, G. *Macromolecules* **1985**, *18*, 1930−1937.
(20) de Boer, A.; Challa, G. *Polymer* **1976**, *17*, 633−637.
(21) Koennecke, K.; Rehage, G. *Makromol. Chem.* **1983**, *184*, 2679−2691.
(22) Koennecke, K.; Rehage, G. *Colloid Polym. Sci.* **1981**, *259*, 1062−1069.
(23) Schomaker, E.; Challa, G. *Macromolecules* **1988**, *21*, 2195−2203.
(24) Schomaker, E.; Hoppen, H.; Challa, G. *Macromolecules* **1988**, *21*, 2203−2209.
(25) Schomaker, E.; Challa, G. *Macromolecules* **1988**, *21*, 3506−3510.
(26) Lemieux, E. J.; Prud'homme, R. E. *Polymer* **1998**, *39*, 5453−5460.
(27) Kusanagi, H.; Tadokoro, H.; Chatani, Y. *Macromolecules* **1976**, *9*, 531−532.
(28) Bosscher, F.; ten Brinke, G.; Challa, G. *Macromolecules* **1982**, *15*, 1442−1444.
(29) Schomaker, E.; Challa, G. *Macromolecules* **1989**, *22*, 3337−3341.
(30) Spevacek, J. *J. Polym. Sci.* **1978**, *16*, 523−528.
(31) Spevacek, J. Schneider, B. *Makromol. Chem.* **1975**, *176*, 729−743.
(32) Spevacek, J.; Schneider, B. *Makromol. Chem.* **1974**, *175*, 2939−2956.
(33) Spevacek, J.; Schneider, B. *Colloid Polym. Sci.* **1980**, *258*, 621−625.
(34) Spevacek, J. *Makromol. Chem., Macromol. Symp.* **1990**, *39*, 71−83.
(35) Dybal, J.; Stokr, J.; Schneider, B. *Polymer* **1983**, *24*, 971−980.
(36) Mori, Y.; Tanzawa, H. *J. Appl. Polym. Sci.*, **1976**, *20*, 1775−1785.
(37) Allen, P. E. M.; Host, D. M.; Truong, V. T.; Williams, D. R. G. *Eur. Polym. J.* **1985**, *21*, 603−610.
(38) Pokorna, V.; Mikes, F.; Pecka, J.; Vyprachticky, D. *Macromolecules* **1993**, *26*, 2139−2140.
(39) Vyprachticky, D.; Pokorna, V.; Pecka, J.; Mikes, F. *Macromolecules* **1997**, *30*, 7821−7827.
(40) Spevacek, J.; Schneider, B. *Adv. Colloid Interface Sci.* **1987**, *27*, 81−150.
(41) te Nijenhuis, K. *Adv. Polym. Sci.* **1997**, *130*, 67−81.
(42) ten Brinke, G.; Schomaker, E.; Challa, G. *Macromolecules* **1985**, *18*, 1925−1930.
(43) Ute, K.; Miyatake, N.; Osugi, Y.; Hatada, K. *Polym. J.* **1993**, *25*, 1153−1160.
(44) Hatada, K.; Ute, K.; Kitayama, T.; Nishiura, T.; Miyatake, N. *Macromol. Symp.* **1994**, *85*, 325−338.
(45) Bosscher, F.; ten Brinke, G.; Eshuis, A.; Challa, G. *Macromolecules* **1982**, *15*, 1364−1368.
(46) White, A. J.; Filisko, F. E. *J. Appl. Phys.* **1982**, *53*, 6563−6567.
(47) Goel, S. K.; Beckman,E. J. *Polym. Eng. Sci.* **1994**, *34*, 1137−1147.
(48) Shimbo, M.; Baldwin, D. F.; Suh, N. P. *Polym. Eng. Sci.* **1995**, *35*, 1387−1393.
(49) Baldwin, D. F.; Shimbo, M.; Suh, N. P. *J. Eng. Mater. Technol.* **1995**, *117*, 62−74.
(50) Kumar, V.; Eddy, S.; Murray, R. *ANTEC* **1996**, 1920−1924.
(51) Baldwin, D. F.; Park, C. B.; Suh, N. P. *Polym. Eng. Sci.* **1996**, *36*, 1437−1445.
(52) Baldwin, D. F.; Park, C. B.; Suh, N. P. *Polym. Eng. Sci.* **1996**, *36*, 1446−1453.
(53) Doroudiani, S.; Park, C. B.; Kortschot, M. T. *Polym. Eng. Sci.* **1996**, *36*, 2645−2662.
(54) Handa, Y. P.; Wong, B.; Zhang, Z.; Kumar, V.; Eddy, S.; Khemani, K. *Polym. Eng. Sci.* **1999**, *39*, 55−61.
(55) Collias, D. I.; Baird, D. G. *Polym. Eng. Sci.* **1995**, *35*, 1167−1177.
(56) Collias, D. I.; Baird, D. G. *Polym. Eng. Sci.* **1995**, *35*, 1178−1183.
(57) Arora, K. A.; Lesser, A. J.; McCarthy, T. J. *Macromolecules* **1998**, *31*, 4614−4620.
(58) Neavor, K. A.; Lesser, A. J.; McCarthy, T. J. *Polym. Prepr.* **1997**, *38*, 446−447.
(59) Kumar, V.; Suh, N. P. *Polym. Eng. Sci.* **1990**, *30*, 1323−1329.
(60) Kumar, V.; Weller, J. E. *Int. Polym. Proc.* **1993**, *8*, 73−80.
(61) Rabinovitch, E. B.; Isner, J. D.; Sidor, J. A.; Wiedl, D. J. *ANTEC* **1997,** 3554−3559.
(62) Patterson, J. *ANTEC* **1997**, 3560−3567.
(63) Matuana, L. M.; Park, C. B.; Balatinecz, J. J. *Cell. Polym.* **1998**, *17*, 1−16.
(64) Goel, S. K.; Beckman, E. J. *Polym. Eng. Sci.* **1994**, *34*, 1148−1156.
(65) Collias, D. I.; Baird, D. G.; Borggreve, R. J. M. *Polymer* **1994**, *35*, 3978−3983.
(66) Seeler, K. A.; Kumar, V. *ANTEC* **1994**, 1972−1976.
(67) Chiou, J. S.; Barlow, J. W.; Paul, D. R. *J. Appl. Polym. Sci.* **1985**, *30*, 3911−3924.
(68) Mizoguchi, K.; Hirose, T.; Naito, Y.; Kamiya, Y. *Polymer* **1987**, *28*, 1298−1302.
(69) Beckman, E.; Porter, R. S. *J. Polym. Sci., Polym. Phys. Ed.* **1987**, *25*, 1511−1517.
(70) Schultze, J. D.; Boehning, M.; Springer, J. *Makromol. Chem.* **1993**, *194*, 339−351.
(71) Handa, Y. P.; Roovers, J.; Wang, F. *Macromolecules* **1994**, *27*, 5511−5516.
(72) Handa, Y. P.; Zhang, Z.; Wong, B. *Macromolecules* **1997**, *30*, 8499−8504.
(73) Zhang, Z.; Handa, Y. P. *Macromolecules* **1997**, *30*, 8505−8507.
(74) Kazarian, S. G.; Briscoe, B. J.; Lawrence, C. J. *ANTEC* **1999**, 2433−2435.
(75) Doroudiani, S.; Park, C. B.; Kortschot, M. T. *ANTEC* **1996**, 1914−1919.
(76) Doroudiani, S.; Park, C. B.; Kortschot, M. T. *Polym. Eng. Sci.* **1998**, *38*, 1205−1215.
(77) Yuki, H.; Hatada, K. *Adv. Polym. Sci.* **1979**, *31*, 1−45.
(78) Kennedy, J. P.; Price, J. L.; Koshimura, K. *Macromolecules* **1991**, *24*, 6567−6571.
(79) Wissinger, R. G.; Paulaitis, M. E. *J. Polym. Sci., Part B: Polym. Phys.* **1991**, *29*, 631−633.
(80) Condo, P. D.; Sanchez, I. C.; Panayiotou, C. G.; Johnston, K. P. *Macromolecules* **1992**, *25*, 6119−6127.
(81) Katime, I.; Quintana, J. R.; Veguillas, J. *Polymer* **1983**, *24*, 903−905.
(82) Yu, J. M.; Jerome, R. *Polymer* **1998**, *39*, 6567−6575.
(83) Kazarian, S. G.; Vincent, M. F.; Bright, F. V.; Liotta, C. L.; Eckert, C. A. *J. Am. Chem. Soc.* **1996**, *118*, 1729−1736.
(84) Bistac, S.; Schultz, J. *Macromol. Chem. Phys.* **1997**, *198*, 531−535.

MA000443N